Vapor–liquid equilibria of the two-dimensional Lennard-Jones fluid(s)

B. Smit
Koninklijke/Shell-Laboratorium, Amsterdam, (Shell Research B.V.) Badhuisweg 3, 1031 CM Amsterdam, The Netherlands

D. Frenkel
FOM-Institute for Atomic and Molecular Physics, Kruislaan 407, 1098 SJ Amsterdam, The Netherlands

(Received 5 November 1990; accepted 18 December 1990)

Monte Carlo simulations in the Gibbs ensemble are presented for the two-dimensional Lennard-Jones fluids. We have considered the full Lennard-Jones potential and the truncated (at 2.5σ) and shifted potential. It is shown that the critical temperature depends largely on the details of the truncation of the potential. These differences are by no means small.

I. INTRODUCTION

Two-dimensional systems are interesting both from a purely theoretical and from an experimental point of view. Examples of real systems that behave effectively as two-dimensional systems are monolayers adsorbed on solid substrates[1] and surfactants adsorbed on an air/water interface.[2]

If a fluid is confined between two parallel plates, the phase behavior of such a system has two limiting cases. For infinite plate separation the system is identical to the three-dimensional bulk system but when the separation between the plates is of the order of a molecular diameter, the fluid behaves like a two-dimensional bulk fluid. In order to study the influence of confinement on the phase behavior it is important to know the phase diagram of the two-dimensional bulk fluid.

The Lennard-Jones potential is given by

$$\phi(r) = 4\epsilon\left[\left(\frac{\sigma}{r}\right)^{12} - \left(\frac{\sigma}{r}\right)^{6}\right], \tag{1}$$

where r is the distance between two particles.

In a simulation the potential is usually truncated at a cutoff radius R^c. The influence of the tail of the potential is usually estimated analytically, by assuming that $g(r) = 1$ for distances greater than the cutoff radius.

If, however, simulations are used to study interfacial properties, this tail correction cannot be added straightforwardly. The simulations are then performed with a truncated potential

$$\Phi(r) = \begin{Bmatrix} \phi(r) & r \leqslant R^c \\ 0 & r > R^c \end{Bmatrix}. \tag{2}$$

The cutoff radius is usually set to $R^c = 2.5\sigma$.

The intermolecular force between a pair of atoms is equal to $-\partial\Phi/\partial r$. Differentiating Eq. (2) with respect to r gives a delta function at $r = R^c$. This delta function is inconvenient in a molecular dynamics simulation. Therefore in a molecular dynamics simulation the potential is not only truncated but also shifted[3]

$$\Phi(r) = \begin{Bmatrix} \phi(r) - \phi(R^c) & r \leqslant R^c \\ 0 & r > R^c \end{Bmatrix}. \tag{3}$$

It turns out that the critical point of the Lennard-Jones fluids modeled with potentials (1), (2), and (3) is different in each case. In this article we study these differences in more detail.

The two-dimensional Lennard-Jones fluid has a vapor–liquid interface that is very rough and foamy.[4] This is caused by the very low interfacial tension[4] of a two-dimensional liquid–vapor interface. In Ref. 5 it is shown that for a simulation in the Gibbs ensemble the interfacial tension is the driving "force" which causes the system to separate into a liquid and vapor phase. It is therefore an interesting question whether for systems with such a small interfacial tension the Gibbs ensemble still yields reliable results for the phase equilibrium properties.

II. COMPUTATIONAL DETAILS

We have used the Gibbs ensemble technique to calculate the vapor–liquid curve of the two-dimensional Lennard-Jones fluids described with Eqs. (1) and (3) with $R^c = 2.5\sigma$. Details on this simulation technique can be found in Refs 6 and 7. A formal proof of the equivalence of the Gibbs ensemble and the canonical ensemble is given in Ref. 5. Our algorithm deviates slightly from the original algorithm of Panagiotopoulos,[6] below we list the main differences.

A convenient method to generate trial configurations in the Gibbs ensemble is to perform a simulation in cycles. One cycle consists (on average) N_{disp} attempts to displace a (random) particle in one of the (randomly chosen) boxes, N_{vol} attempts to change the volume of the subsytems, and N_{try} attempts to exchange particles between the boxes. It is important to ensure that at each step of the simulation the condition of detailed balance is fulfilled.

In most published applications of the Gibbs ensemble the simulations are performed somewhat differently; instead of making a random choice at each Monte Carlo step of the type of trial move to be made (particle displacement, volume change, or particle exchange), the trial moves are carried out sequentially. First, trial displacements are attempted for each particle successively (the "N,V,T part"), then a trial move to change the volume is carried out (the "N,P,T part"), and finally one performs N_{try} attempts to exchange particles (the "μ,V,T part"). Although with this scheme microscopic reversibility is not guaranteed, it can be expected that this method of generating new configurations will

Downloaded 17 Aug 2004 to 134.174.142.154. Redistribution subject to AIP license or copyright, see http://ojps.aip.org/jcpcr/jcpcr.jsp

also lead to the correct probability distribution. However, the "random" scheme used in the present work has some practical advantages. For example, there is no ambiguity when to gather data for subsequent analysis. In contrast, with sequential where sampling a choice must be made whether to sample after the N,V,T part, the N,P,T part, or the μ,V,T part.

A more serious disadvantage of the sequential method was noted by Panagiotopoulos:[6] erroneous results can occur, when the probability of acceptance of an exchange becomes greater than 3%. In Ref. 6, a bias in the liquid pressure was observed, which disappeared when the number of attempts to exchange particles was reduced. It seems likely that this problem is due to trapping of the system in a pocket of configuration space. The nature of the "metastable" fluctuations was discussed at length in Ref. 5.

We performed several tests to compare the results obtained with the random and sequential methods. Not surprisingly, the extra time needed to select the type of trial move is negligible. With the random sampling, less simulations became trapped in metastable regions than with the corresponding sequential scheme. Furthermore, the standard deviation of the chemical potential was significantly smaller. Since the chemical potential (see Ref. 8 for the formula of the chemical potential in the Gibbs ensemble) is calculated during the exchange step, a large number of successful exchanges could bias the results for the chemical potential in case of the successive scheme.

In Refs. 6 and 7 a new configuration in the volume step is generated by making a random walk in V_1. A more natural choice for generating a new configuration in the volume change step, is to make a random walk in $\ln[V_1/(V-V_1)]$, instead of in V_1 (see Ref. 9 for the N,P,T ensemble). This has the advantage that the domain of this random walk coincides with the possible values of V_1. Furthermore, the average step size turns out to be less sensitive to the density.

In order to adopt this method for the Gibbs ensemble, the acceptance rule for the volume has to be modified (see also Ref. 9). For a random walk in $\ln[V_1/(V-V_1)]$ we have for an ensemble average in the Gibbs ensemble[8,10]

$$\langle f(\xi^N)\rangle = \frac{1}{Q_{N,V,T}}\frac{1}{\Lambda^{3N}N!}\sum_{n_1=0}^{N}\binom{N}{n_1} \times\int_{-\infty}^{\infty} d\left[\ln\left(\frac{V_1}{V-V_1}\right)\right]\frac{V_1(V-V_1)}{V} \times V_1^{n_1}(V-V_1)^{N-n_1}\int d\xi_1^{n_1}\exp[-\beta U_1(n_1)] \times\int d\xi_2^{N-n_1}\exp[-\beta U_2(N-n_1)]f(\xi^N), \tag{4}$$

in which $Q_{N,V,T}$ is the partition function in the Gibbs ensemble[8,11]

$$Q_{N,V,T}\equiv\frac{1}{\Lambda^{3N}N!}\sum_{n_1=0}^{N}\binom{N}{n_1}\int_0^V dV_1\, V_1^{n_1}(V-V_1)^{N-n_1} \times\int d\xi_1^{n_1}\exp[-g\beta U_1(n_1)]\int d\xi_2^{N-n_1} \times\exp[-\beta U_2(N-n_1)], \tag{5}$$

and where $\xi_1 = \mathbf{r}/L$ is the scaled coordinates of a particle, L is the box length of the subsystem in which the particle is located, n_1 denotes the number of particles in box 1, V_1 denotes the volume of box 1, Λ is the thermal de Broglie wavelength, $\beta = 1/k_BT$, and $U(n_i)$ is the intermolecular potential.

In Eq. (4) we recognize a pseudo-Boltzmann factor

$$\exp[-\beta W]\equiv\exp\left[\ln\binom{N}{n_1}+(1+n_1)\ln V_1 + (1+N-n_1)\ln(V-V_1)-\ln V - \beta U_1(n_1)-\beta U_2(N-n_1)\right]. \tag{6}$$

From this equation we can derive straightforwardly the acceptance rule for the volume step[8]

$$\Delta W = (U_1''-U_1')+(U_2''-U_2') - \frac{(n_1+1)}{\beta}\ln\left(\frac{V_1''}{V_1'}\right)-\frac{(N-n_1+1)}{\beta}\ln\left(\frac{V-V_1''}{V-V_1'}\right), \tag{7}$$

where superscript $''$ denotes the new configuration and superscript $'$ denotes the old configuration. The acceptance rules for the displacement of a particle and a particle exchange are not affected.

III. RESULTS AND DISCUSSION

A. The full Lennard-Jones potential

The two-dimensional Lennard-Jones fluid has been studied using conventional simulation techniques by several authors.[4,12-22] The equation-of-state data of these simulations together with additional data from conventional Monte Carlo simulations and the virial equation of state were fitted to a 33 parameter Benedict–Webb–Rubin equation by Reddy and O'Shea.[23] From this equation of state they obtained as estimates for the critical temperature and density $T_c = 0.537$ and $\rho_c = 0.365$.

This estimate of the critical temperature disagrees with recent results of Singh *et al.*,[24] who used the Gibbs ensemble technique to determine parts of the vapor liquid curve for the two-dimensional Lennard-Jones fluid [as given by Eq. (1), the potential is truncated at half the box size and the long-tail corrections are estimated by assuming $g(r) = 1$ for distances greater than have the bixe size]. The data of Ref. 24 were fitted to a scaling law for the density, using the critical exponent of the two-dimensional Ising system ($\beta = 1/8$). This procedure yielded an estimate for the critical temperature and density: $T_c = 0.472$ and $\rho_c = 0.33 \pm 0.02$.

We have repeated the Gibbs ensemble simulations of Singh *et al.* The results of our simulation are presented in Fig. 1 and Table I. If we fit our results to the scaling law for the density (using the two-dimensional Ising critical exponent) and to the law of rectilinear diameters,[10] we obtain the following estimates for the critical temperature and density $T_c = 0.515 \pm 0.002$ and $\rho_c = 0.355 \pm 0.003$. These results are in good agreement with the results of Gibbs ensemble

Downloaded 20 Aug 2001 to 145.18.129.54. Redistribution subject to AIP license or copyright, see http://ojps.aip.org/jcpo/jcpcr.jsp

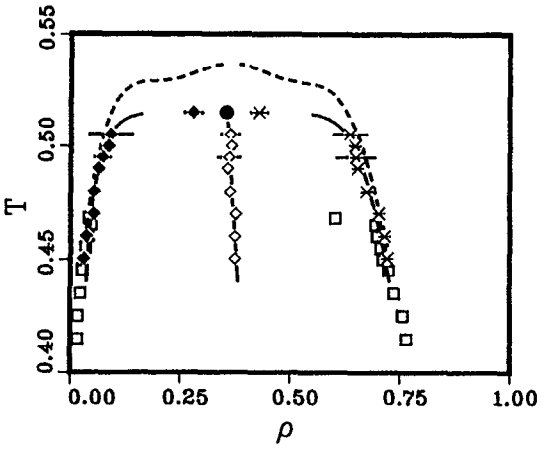

FIG. 1. Phase diagram of the (full) two-dimensional Lennard-Jones fluid. The full lines are the fits to the scaling law and the rectilinear law. The dashed line is the equation of state of Reddy and O'Shea (Ref. 23). □ are the Gibbs ensemble results of Singh *et al.* (Ref. 24). ×, ◇, and ⊕ are the Gibbs ensemble results of this work. ● is the estimate of the critical point on the basis of the simulation results.

simulations of Nicolaides[25] who obtained $T_c = 0.522 \pm 0.002$ and $\rho_c = 0.366 \pm 0.009$.

The phase diagram obtained from the equation of state of Reddy and O'Shea (see Fig. 1), is in reasonable agreement with our Gibbs ensemble simulation results far away from the critical point. Close to the critical point, the equation-of-state exhibits a strange "hump." This seems to be an artefact of the equation-of-state of Ref. 23. In two-dimensional systems the coexistence curve is very flat near the critical point. This behavior cannot be described by an analytic equation of state. A 33 parameter equation has sufficient flexibility to enforce some of this "flatness." Close to the critical point, however, such an equation of state yields a coexistence curve that is characterized by the classical exponent $\beta = 1/2$, which results in a hump in the coexistence curve.

It is instructive to look at the data of Singh *et al.* more carefully (see Fig. 1). These authors fit their simulation data on the coexistence densities to a function that correctly reproduces the extremely flat top described by the two-dimensional Ising exponent $\beta = 1/8$. As a consequence the estimate of the critical temperature depends sensitively on the data collected just below the critical point. Unless data have been collected very close to the critical point, it is almost impossible to obtain an accurate estimate of T_c. It seems plausible that such an extrapolation error is at the root of the discrepancy between the estimate of T_c in Ref. 24 and the value obtained by Reddy and O'Shea[23] and the present results. In fact, Singh *et al.* report no data point above $T = 0.470$. Figure 1 shows that except for the point at $T = 0.47$ our simulation results are in excellent agreement with the results of Singh *et al.*

In Fig. 2 we have plotted an histogram of the densities measured during a simulation in the Gibbs ensemble at $T = 0.49$. This figure clearly shows that above $T = 0.472$ one can observe vapor–liquid coexistence. In Fig. 3 we have plotted the same histogram, but now for $T = 0.51$. This figure exhibits three peaks, which is an indication (see Sec. IV and Ref. 5) that the system is very close to the critical temperature.

B. The truncated and shifted potential

The results for the truncated and shifted potential [Eq. (3)] are presented in Fig. 4 and Table II. The estimated critical point is $T_c = 0.459 \pm 0.001$ and $\rho_c = 0.35 \pm 0.01$. Comparison with the phase diagram of the full two-dimensional Lennard-Jones potential (Fig. 4) shows that the influence of the tail of the potential is substantial. Similar behavior has also been observed in the three-dimensional Lennard-Jones fluid.[26,27]

Our finding of this large difference between the full and truncated two-dimensional Lennard-Jones models is at odds with the observation of Sikkenk *et al.*[4,21] who could not detect differences between the two model systems.

The influence of the truncation of the potential can be estimated from the equation of state of Reddy and O'Shea by

TABLE I. Results for the (full) two-dimensional Lennard-Jones fluid. N is the total number of particles, T is the temperature, N_{cy} is the number of Monte Carlo cycles, ρ is the density, P is the pressure, E is the energy, and μ is the chemical potential. The number of attempts per cycle to insert a particle were: for $N = 108$; $N_{try} = 40$, for $N = 216$; $N_{try} = 100$, and for $N = 512$; $N_{try} = 250$. The small subscripts give the accuracy of the last digit(s), so 0.731_7 means 0.731 ± 0.007.

			Gas phase				Liquid phase			
N	T	$\frac{N_{cy}}{10^3}$	ρ_g	P_g	$-E_g$	$-\mu_g$	ρ_l	P_l	$-E_l$	$-\mu_l$
108	0.450	10	0.030_9	0.011_3	0.3_2	1.77_{16}	0.722_9	0.01_3	2.26_4	1.82_{27}
108	0.460	10	0.036_9	0.012_2	0.3_2	1.76_{14}	0.72_1	0.01_2	2.23_5	1.82_{51}
216	0.470	10	0.05_2	0.017_4	0.45_5	1.72_{13}	0.70_1	0.01_2	2.19_5	1.73_{26}
216	0.480	10	0.053_6	0.017_2	0.4_1	1.74_6	0.68_2	0.01_1	2.11_3	1.71_{15}
216	0.490	10	0.064_8	0.020_2	0.5_1	1.72_5	0.65_1	0.02_2	2.05_3	1.69_{14}
216	0.495	10	0.07_2	0.021_2	0.6_4	1.70_6	0.65_4	0.02_2	2.00_7	1.71_{17}
216	0.500	10	0.09_2	0.024_2	0.6_3	1.70_6	0.65_1	0.03_1	2.03_7	1.71_{16}
216	0.505	10	0.09_1	0.027_6	0.9_6	1.69_8	0.64_1	0.03_2	2.0_3	1.66_{11}
512	0.515	3	0.28_2	0.026_8	...[a]	1.68_{13}	0.43_2	0.03_1	...[a]	1.71_{18}

[a] The boxes changed identity during the simulation.

Downloaded 20 Aug 2001 to 145.18.129.54. Redistribution subject to AIP license or copyright, see http://ojps.aip.org/jcpo/jcpcr.jsp

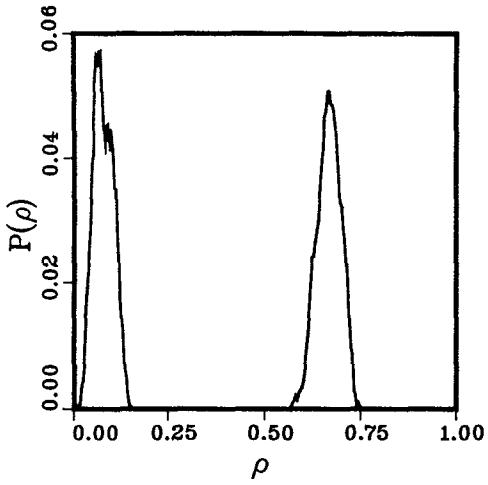

FIG. 2. Density probability function for the two-dimensional Lennard-Jones fluid at $T = 0.490$. The curve gives the probability of finding the density ρ in one of the boxes in the Gibbs ensemble.

subtracting the tail correction[26]

$$p_{\mathrm{tr}2d} = p_{\mathrm{LJ}2d}(T,\rho) + \frac{3\pi\rho^2}{(R^c)^4}, \tag{8}$$

where $p_{\mathrm{tr}2d}$ is the pressure of the truncated and shifted two-dimensional Lennard-Jones fluid and $p_{\mathrm{LJ}2d}$ is the equation of state of Reddy and O'Shea. Figure 4 shows that this corrected equation of state works well below $T = 0.45$. The critical temperature ($T_c = 0.454$), however, is underestimated considerably.

C. The truncated but *un*-shifted potential

The truncated but *un*-shifted potential is considered by Rovere *et al.*[28,29] These authors use finite-size scaling techniques to estimate the critical temperature. Rovere *et al.* estimate a critical temperature $T_c = 0.50 \pm 0.02$.

It would be interesting to make a comparison of the results of Gibbs ensemble simulations with the results from the finite-size scaling techniques. This would elucidate whether the conjecture that the Gibbs ensemble yields a better estimate of the critical point than conventional simulation techniques[5] is indeed true.

IV. FINITE-SIZE EFFECTS

The finite-size effects can be estimated by calculating the probability of the formation of droplets of gas or liquid in the two boxes using the method described in,[5] by replacing the formula with expressions for a two-dimensional system.[27]

This probability is given by

$$P(\rho) = \frac{\iint_S dx\,dy\,\delta\left(\frac{x}{y} - \rho\right)\exp[-\beta F_{\mathrm{surf}}(x,y)]}{\iint_S dx\,dy\,\exp[-\beta F_{\mathrm{surf}}(x,y)]}, \tag{9}$$

where $x = n_1/N$, $y = V_1/V$ and $F_{\mathrm{surf}}(x,y)$ is the surface contribution to the free energy. This surface contribution can be estimated from

$$F_{\mathrm{surf}}(x,y) = \gamma A(x,y), \tag{10}$$

where ρ is the density in one of the boxes, γ is the interfacial tension and $A(x,y)$ the total (minimal) surface area for a given x, y (for a two-dimensional system this can either be a 'circle' of gas, 'circle' of liquid, or a double line).

The interfacial tension at a given temperature is estimated with the scaling law for the surface tension[30]

$$\gamma = \gamma_0\left(1 - \frac{T}{T_c}\right)^{\mu}, \tag{11}$$

with a two-dimensional Ising critical exponent [$\mu = 1$ (Ref. 30)].

We have calculated γ_0 using the results of Sikkenk *et al.*[4,22] who estimated the surface tension of the two-dimensional Lennard-Jones fluid using capillary wave theory. At $T = 0.427$ they obtained: $\gamma = 0.05 \pm 0.01$. In Refs. 4 and 22 it is mentioned that the model that was simulated corresponds to a two-dimensional truncated Lennard-Jones system [Eq. (2)]. As the results in Refs. 4 and 22 were obtained by the molecular dynamics technique, the potential must, in fact, have been shifted as well as truncated [Eq. (3)]. How-

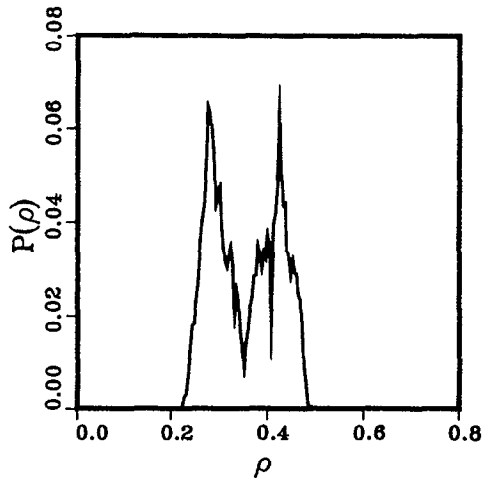

FIG. 3. Density probability function for the two-dimensional Lennard-Jones fluid at $T = 0.510$ (see also the caption to Fig. 2).

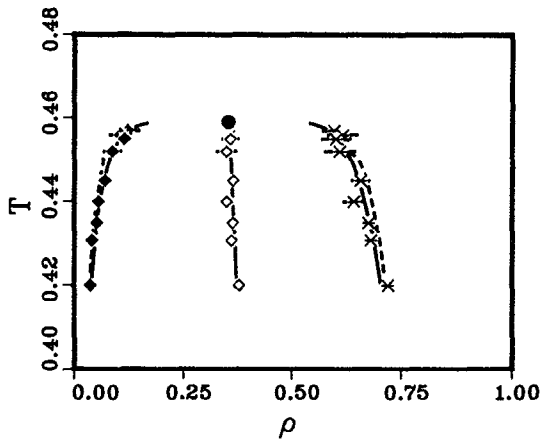

FIG. 4. Phase diagram of the truncated and shifted two-dimensional Lennard-Jones fluid. The dashed line is the corrected equation of state (8). See also the caption to Fig. 1.

Downloaded 20 Aug 2001 to 145.18.129.54. Redistribution subject to AIP license or copyright, see http://ojps.aip.org/jcpo/jcpcr.jsp

TABLE II. Results for the truncated and shifted two-dimensional Lennard-Jones fluid (1) (see caption to Table I).

			Gas phase				Liquid phase			
N	T	$\frac{N_{cy}}{10^3}$	ρ_g	P_g	$-E_g$	$-\mu_g$	ρ_l	P_l	$-E_l$	$-\mu_l$
512	0.420	4	0.037_5	0.010_2	0.4_1	1.63_7	0.72_2	0.01_2	2.13_5	1.68_{27}
512	0.431	4	0.040_2	0.010_2	0.4_1	1.61_6	0.68_2	0.01_2	2.06_5	1.60_{20}
512	0.435	4	0.052_6	0.014_1	0.4_1	1.61_6	0.676_6	0.06_{17}	2.02_4	1.61_{20}
512	0.440	4	0.055_7	0.015_2	0.5_1	1.61_4	0.64_2	0.00_1	2.00_4	1.60_{19}
512	0.445	6	0.07_1	0.017_2	0.6_2	1.59_4	0.66_2	0.017_9	1.96_5	1.61_{16}
512	0.455	4	0.11_1	0.022_4	0.9_3	1.57_{10}	0.60_3	0.022_{15}	1.85_7	1.58_{12}
512	0.456	7	0.11_2	0.021_2	0.9_4	1.58_5	0.62_2	0.022_8	1.9_1	1.56_{15}
512	0.457	12	0.12_3	0.020_2	0.9_3	1.59_{13}	0.60_3	0.021_8	1.9_1	1.57_5

ever, the estimate of the critical temperature ($T_c = 0.533$), that was used in Refs. 4 and 22 is based on the results of Barker *et al.*,[17] who considered the *full* Lennard-Jones potential [Eq. (1)]. As was shown above, this estimate is not appropriate for the truncated-and-shifted two-dimensional Lennard-Jones model. We have therefore not used this value for the critical temperature to estimate γ_0. Rather, we used the results of the Gibbs ensemble simulations for the truncated and shifted potential (2), which gave $T_c = 0.459$. Note that with $T_c = 0.53$ the estimate of γ_0 would have been four times smaller, such a small surface tension would imply that simulations in the Gibbs ensemble would be impossible for this fluid in the temperature range that we have studied.

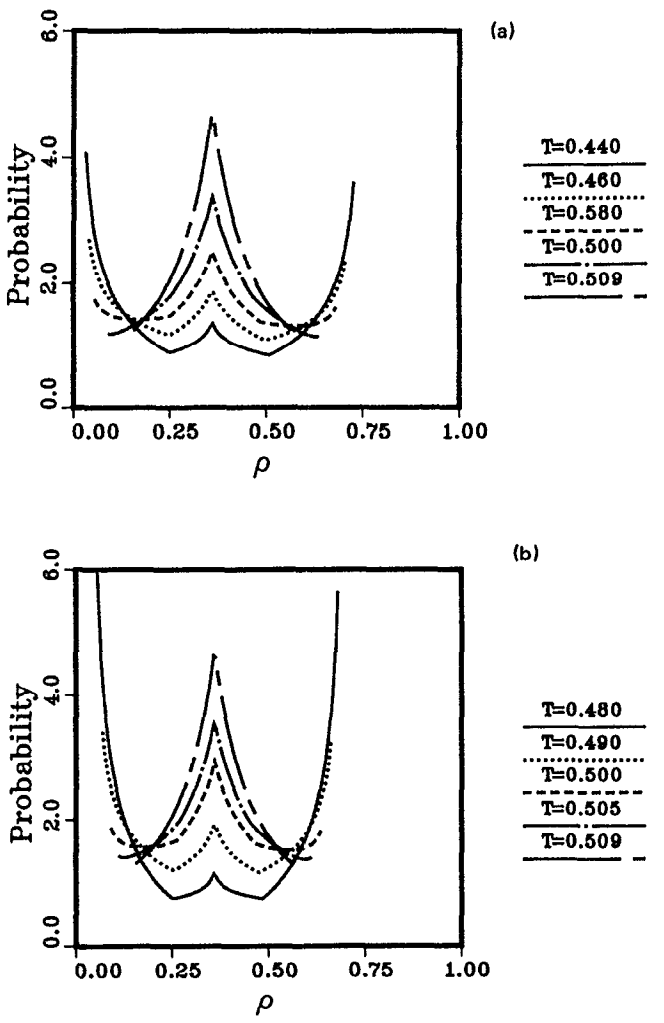

FIG. 5. Calculated density probability function for the two-dimensional Lennard-Jones fluid for various numbers of particles [(a) $N = 64$ and (b) $N = 512$]. Note that we have assumed that the critical temperature is independent of the number of particles.

In Fig. 5 the calculated probability distributions are shown. This distribution gives the probability of finding the density ρ in one of the boxes. In Ref. 5 it is shown that for the Gibbs ensemble these figures have a typical behavior close to the critical temperature. Well below the critical temperature two separate peaks, corresponding to the liquid and vapor densities, can be observed. Close to the critical point a third peak, which corresponds to the overall density can be observed. This peak originates from entropic effects. Due to the low surface tension close to the critical point, it becomes for the system possible to form droplets of liquid or gas, which give rise to the third peak.

The Fig. 5 shows that for a system with 512 particles finite-size effects (for example the occurrence of a third peak) can be expected for $0.96T_c < T < T_c$. For a system with only 64 particles finite-size effects can be expected for $0.9T_c < T < T_c$. The finite size-effects are sufficiently small to obtain a reliable estimate of the critical point.

V. CONCLUDING REMARKS

In this paper we have demonstrated by numerical simulation the very strong effect on the phase diagram caused by small changes in the treatment of the long-range part of the Lennard-Jones potential. As direct simulation of the untruncated Lennard-Jones potential is extremely uneconomical, different authors have used different truncation procedures. For many bulk properties the nature of the truncation makes little difference. For the liquid–vapor coexistence curves, however, these seemingly small changes in truncation procedure make a very large difference indeed. This is not sufficiently realized by many authors. As a consequence, the literature abounds with examples where confusing results are obtained because data obtained with different "Lennard-Jones" potentials are mixed up. In this paper we have calcu-

Downloaded 20 Aug 2001 to 145.18.129.54. Redistribution subject to AIP license or copyright, see http://ojps.aip.org/jcpo/jcpcr.jsp

lated the vapor–liquid curve of various two-dimensional Lennard-Jones fluids using the Gibbs ensemble technique, in order to quantify this effect and to provide future authors with reference data for the most frequently used versions of the Lennard-Jones potential.

ACKNOWLEDGMENTS

The authors would like to acknowledge the contributions of M. P. Allen, E. M. Hendriks, D. Nicolaides, M. Rovere, J. H. Sikkenk, Ph. de Smedt, and D. J. Tildesley. The work of the FOM Institute is part of the research program of FOM and is supported by "Nederlandse Organisatie voor Wetenschappelijk Onderzoek" (NWO).

[1] W. A. Steele, *The Interaction of Gases with Solid Surfaces* (Pergamon, Oxford, England, 1974).
[2] D. J. Shaw, *Introduction to Colloid and Surface Chemistry* (Butterworths, London, 1980).
[3] In some studies the discontinuity of the first derivative of the potential is also removed by introducing $\alpha r^2 + \beta$ as an extra term in the potential.
[4] J. H. Sikkenk, PhD thesis, Rijksuniversiteit Leiden, The Netherlands, 1987.
[5] B. Smit, Ph. de Smedt, and D. Frenkel, Mol. Phys. **68**, 931 (1989).
[6] A. Z. Panagiotopoulos, Mol. Phys. **61**, 813 (1987).
[7] A. Z. Panagiotopoulos, N. Quirke, M. Stapleton, and D. J. Tildesley, Mol. Phys. **63**, 527 (1988).
[8] B. Smit and D. Frenkel, Mol. Phys. **68**, 951 (1989).
[9] R. Eppinga and D. Frenkel, Mol. Phys. **52**, 1303 (1984).
[10] B. Smit and C. P. Williams, J. Phys. Condens. Matter **2**, 4281 (1990).
[11] D. Frenkel, in *Computer Modelling of Fluids, Polymers and Solids*, edited by C. R. A. Catlow, Proc. NATO ASI (Kluwer Academic, Dordrecht, 1990).
[12] P. L. Fehder, J. Chem. Phys. **50**, 2617 (1969).
[13] F. Tsien and J. P. Valeau, Mol. Phys. **27**, 177 (1974).
[14] S. Toxvaerd, Mol. Phys. **29**, 373 (1975).
[15] W. A. Steele, J. Chem. Phys. **65**, 5256 (1976).
[16] D. Henderson, Mol. Phys. **34**, 301 (1977).
[17] J. A. Barker, D. Henderson, and F. F. Abraham, Physica A **106**, 226 (1981).
[18] J. M. Phillips, L. W. Bruch, and R. D. Murphy, J. Chem. Phys. **75**, 5097 (1981).
[19] C. Bruin, A. F. Bakker, and M. Bishop, J. Chem. Phys. **80**, 5859 (1984).
[20] J. Tobochnik and G. V. Chester, Phys. Rev. B **25**, 6778 (1982).
[21] J. H. Sikkenk, H. J. Hilhorst, and A. F. Bakker, Physica A **131**, 587 (1985).
[22] J. H. Sikkenk, J. M. J. van Leeuwen, E. O. Vossnack, and A. F. Bakker, Physica A **146**, 622 (1987).
[23] M. R. Reddy and S. F. O'Shea, Can. J. Phys. **64**, 677 (1986).
[24] R. R. Singh, K. S. Pitzer, J. J. De Pablo, and J. M. Prausnitz, J. Chem. Phys. **92**, 5463 (1990).
[25] D. Nicolaides, M. P. Allen, and D. J. Tildesley (private communications).
[26] J. E. Finn and P. A. Monson, Phys. Rev. A **39**, 6402 (1989).
[27] B. Smit, PhD thesis, Rijksuniversiteit Utrecht, The Netherlands, 1990.
[28] M. Rovere, D. W. Hermann, and K. Binder, Europhys. Lett. **6**, 585 (1988).
[29] M. Rovere, D. W. Hermann, and K. Binder, J. Phys. Condens. Matter **2**, 7009 (1990).
[30] J. S. Rowlinson and B. Widom, *Molecular Theory of Capillarity* (Clarendon, Oxford, 1982).

Downloaded 20 Aug 2001 to 145.18.129.54. Redistribution subject to AIP license or copyright, see http://ojps.aip.org/jcpo/jcpcr.jsp